Copper Oxide–Based Model of Persistent Free Radical Formation on Combustion-Derived Particulate Matter

ARTICLE *in* ENVIRONMENTAL SCIENCE AND TECHNOLOGY · AUGUST 2008

Impact Factor: 5.33 · DOI: 10.1021/es071708h · Source: PubMed

4 AUTHORS, INCLUDING:

Slawo M. Lomnicki
Louisiana State University
74 PUBLICATIONS **881** CITATIONS

SEE PROFILE

Eric Vejerano
Virginia Polytechnic Institute and State Uni…
17 PUBLICATIONS **192** CITATIONS

SEE PROFILE

Barry Dellinger
Louisiana State University
145 PUBLICATIONS **2,304** CITATIONS

SEE PROFILE

Environ. Sci. Technol. **2008,** *42,* 4982–4988

Copper Oxide-Based Model of Persistent Free Radical Formation on Combustion-Derived Particulate Matter

SLAWO LOMNICKI, HIEU TRUONG, ERIC VEJERANO, AND BARRY DELLINGER*

Department of Chemistry, 413 Choppin Hall, Louisiana State University, Baton Rouge, Louisiana 70803

Received July 11, 2007. Revised manuscript received December 11, 2007. Accepted February 7, 2008.

We have found that environmentally persistent free radicals (PFRs) are formed by adsorption of substituted aromatic molecular precursors on the surface of cupric oxide-containing particles at temperatures between 100 and 400 °C. This temperature range corresponds to the conditions in the postflame, cool zone of combustion, and thermal processes. Depending upon the nature of the precursor and the adsorption temperature, both substituted phenoxyl and semiquinone radicals are formed. The PFRs are formed through a mechanism of initial physisorption, followed by chemisorption via elimination of water or hydrogen chloride, and electron transfer resulting in the simultaneous reduction of Cu(II) to Cu(I) and formation of the PFR. The PFRs are still observable by electron paramagnetic resonance (EPR) after exposure to air for more than a day. Their lifetimes under vacuum appear to be infinite. Other redox-active transition metals such as iron are expected to also mediate or catalyze the formation of PFRs. The properties of the observed radicals are consistent with radicals previously observed on airborne and combustion-generated particulate matter. We propose a catalytic biochemical cycle for both the particle-associated semiquinone and phenoxyl PFRs that result in the formation of hydroxyl radical and other reactive oxygen species (ROS). This suggests that combustion-generated, particle-associated PFRs may be responsible for the oxidative stress resulting in cardiopulmonary disease and probably cancer that has been attributed to exposure to airborne fine particles.

Introduction

Epidemiological studies indicate that >500,000 people die yearly in the U.S. from cardiopulmonary disease due to exposure to fine particle air pollution, and possibly even more die due to induction of cancer (*1, 2*). Initially, research focused on the irritation caused by the fine particle fraction defined by the Environmental Protection Agency (EPA) as PM2.5 (particulate matter, PM, with a mean aerodynamic diameter of less than 2.5 μm). However, ultrafine particles (PM0.1, or particles with a mean aerodynamic diameter of less than 0.1 μm) comprise over 50% of PM2.5 by mass and 99.9% by number distribution, and physiological responses to particle exposure are likely to be due to ultrafines (*3, 4*). The source of toxicity of these particles is not clear and is the subject of considerable scientific debate (*5, 6*).

Characterization of airborne fine and ultrafine particles suggest that over 70 and 90% are produced in combustion sources, respectively (*7, 8*). Some of this fraction is the result of secondary atmospheric reactions in which sulfur dioxide emissions are converted to sulfates that serve as condensation nuclei for particle formation/growth and possible condensation of various chemicals (*9*). The primary combustion-generated, ultrafine particles consist of elemental carbon (e.g., soot); inorganic species such as silica, alumina, and sulfates; trace metals and transition metals; and organic compounds (*7–10*).

The biomedical research community has generated evidence that the health impacts of ultrafine particles are primarily due to oxidative stress in which the body's defense mechanisms "overrespond" to exogenous stimuli (*5, 11, 12*). Oxidative stress is induced by "reactive oxygen species" (ROS) that include hydrogen peroxide, superoxide, and hydroxyl radical (*13*). Fe^{2+} ions in solution can promote ROS production through the well-known Fenton reaction (*13*). Since iron is usually the dominant transition metal in combustion-generated particles, research has focused on the role of iron in ROS production (*14*). However, iron exists as Fe^{3+} rather than Fe^{2+} in particulate matter and is not mobile in solution as is seemingly required for the Fenton reaction to be a viable source of particle-induced oxidative stress (*15*).

We have previously demonstrated that airborne and combustion-generated particles contain environmentally persistent free radicals (PFRs) that exist indefinitely on some types of particles. The particles induce damage to DNA that can be attributed to free radicals (*16–18*). We have argued that the EPR spectra and persistence of these PFRs are consistent with those of semiquinone-type radicals that are known to be stable and resistant to oxidation and can induce formation of ROS in biological systems. We have previously proposed that these PFRs are formed by a mechanism of physisorption of the molecular precursor, followed by chemisorption at a metal oxide surface site, and electron transfer to the metal to form a surface-associated PFR and the reduced metal (cf. Figure A, Supporting Information) (*19–21*). However because of the nonuniformity of airborne PM, the assignment of the structure of these radicals, their origin, and reasons for their stability/nonreactivity cannot be confirmed. We now report the results of a detailed laboratory study of the formation, structure, and persistence of PFRs formed from various molecular precursors on a particle substrate of 5% CuO on silica.

Materials and Methods

CuO was selected because of its known redox properties and documented catalysis of the formation of dioxins in combustion systems, and our previous research has inferred the formation of PFRs and their role as reaction intermediates in the pathway of formation of dioxins over this surface (*19, 21–23*). Silica is a common inorganic material in combustion-generated PM and serves as an inert substrate to facilitate control of the CuO concentration and sample handling; 5% CuO is higher than the typical concentrations of copper reported in combustion-generated and airborne PM and was primarily used for comparison to the dioxin literature. However, the emerging data on transition metals suggest that this concentration may be appropriate for

* Corresponding author phone: 225 578-6759; fax: 225 578-0276; e-mail: barryd@lsu.edu.

10.1021/es071708h CCC: $40.75

Published on Web 05/14/2008

ultrafine PM where the concentration of metals increases with decreasing particle size (*10*).

The molecular precursors chosen for study were the substituted benzenes: hydroquinone (HQ), catechol (CT), phenol (P), 2-chlorophenol (2-MCP), monochlorobenzene (MCBz), and 1,2-dichlorobenzene (1,2-DCBz). Hydroquinone and catechol were chosen because they are known precursors of semiquinone radicals, and our research on dioxin formation suggested that they are formed on CuO surfaces (*19, 21, 24*). Phenol is the most common partial oxidation product of aromatic species in combustion systems (*25*). 2-MCP, MCBz, and 1,2-DCBz are all chlorinated aromatics that are suspected dioxin precursors that react with silica or CuO surfaces to produce chemisorbed species (*25, 26*).

Particulates of 5% CuO supported on silica were prepared by impregnation of silica gel with copper nitrate hemipentahydrate using the method of incipient wetness followed by calcination. The silica gel powder (Sigma-Aldrich, grade 923 100–200 mesh) was introduced into a 0.1 M solution of the copper nitrate (Sigma-Aldrich, copper(II) nitrate hemipentahydrate, 99+%). The samples were allowed to gel for 24 h at room temperature and dried at 120 °C for 12 h before calcination in air for 5 h at 450 °C. The resulting powder was ground and sieved to 100–120 mesh (mean particle diameter of 125–150 μm). The adsorbate chemicals, HQ (Sigma, 99+%), CT (Aldrich, 99+%), P (Aldrich, 99+%), 2-MCP (Aldrich, 99+%), MCBz (Aldrich, 99.8% anhydrous), and 1,2-DCBz (Sigma-Aldrich, 99% HPLC grade) were used without further purification.

The particulate samples were exposed to the vapors of the adsorbates using a custom-made vacuum exposure system presented in Figure B in the Supporting Information that consisted of a vacuum gauge, dosing vial port, equilibration chamber, and two reactors. Each sample was reoxidized in situ in air at 450 °C and then evacuated to 10^{-2} torr. The particles were dosed with adsorbate vapors at 10 torr at the desired temperature (150−400 °C) for 5 min. The port and dosing tube were evacuated for 1 h at the dosing temperature and 10^{-2} torr to remove any residual physisorbed dosant. The reactor was then sealed under vacuum with a vacuum-tight PFE stopcock and allowed to cool to room temperature.

Electron paramagnetic resonance (EPR) measurement were performed using a Bruker EMX-20/2.7 spectrometer at a microwave power of 1 mW, 9 GHz frequency, 4 G amplitude, and 100 kHz frequency. The spectra were subjected to spectral deconvolution as nonderivative spectra using the Origin 7E Peak Fitting module, and the overall fit was compared with both the original absorption spectra and first derivative spectra.

Results and Discussion

EPR analyses of the undosed $Cu^{II}O$/silica revealed a broad signal (300 G) originating from the unpaired electron in copper. After dosing, a narrow EPR spectrum, typical of organic radicals, was superimposed on the broad metal ion signal. This signal slowly diminished over a period of days when exposed to air, indicating that highly persistent free radicals were formed (cf. Figure 1).

Figure 2 depicts the first derivative EPR spectra of PFRs observed for various adsorbates as a function of dosing temperature. The spectra are complex and asymmetrical, indicating the presence of more than one type of radical. Mathematical deconvolution of the spectra resulted in the assignment of the EPR absorption bands (cf. Figure C in the Supporting Information). Table 1 summarizes the values of the *g*-factors for each adsorbate at 150 and 300 °C.

For 1,2-DCBz, MCBz, and phenol, the total number of radicals increased to a maximum at 200–230 °C, followed by a rapid decrease as the dosing temperature was increased

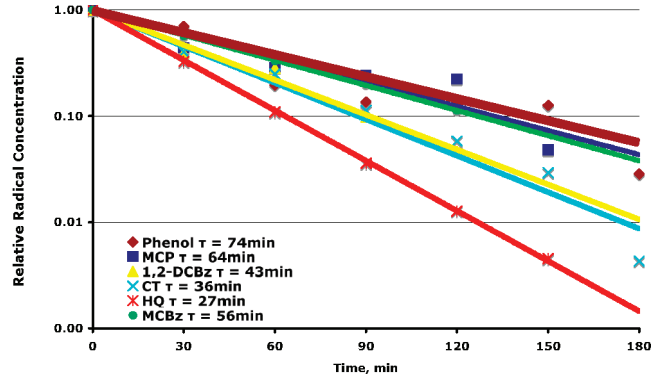

FIGURE 1. First-order decay (normalized) and 1/e lifetimes (τ) of EPR signals resulting from the dosing of 5% $Cu^{II}O$/silica particles with various radical precursors at 230 °C and exposed to air at room temperature.

(cf. Figure 3). For CT, HQ, and 2-MCP the overall number of radicals increased with increasing dosing temperature. This behavior is related to the stability and interconversion of the PFRs (vide infra).

In our model of PFR formation, the interaction of the organic molecules with the surface of metal oxides leads to the formation of a chemisorbed organic−CuO complex that undergoes electron transfer to form surface-associated PFRs. As a result of electron transfer, the metal is reduced, and an EPR F-center is produced. Depending on the structure of the adsorbate and the nature of the surface adsorption site, we believe phenoxyl- and/or semiquinone-type PFRs are formed with characteristic EPR *g*-factors of 2.0030–2.0050 (g2) and 2.0060–2.0070 (g3), respectively.

Particle F-Center Formation. Spectral deconvolution of the EPR absorption spectra of the copper oxide/silica samples before and after dosing indicates the presence of an EPR signal with a constant, low *g*-value of 2.0010–2.0020 (g1). In our model of PFR formation, the electron is transferred from the adsorbate to the metal ion center. This may result in an electron trapped in the solid matrix that forms an F-center that is the source of g1. Indeed F-centers are known and broadly described in the literature as an electron trapped in the anionic vacancy of the metal oxide and exhibit very low *g*-values of 2.0011–2.0020 (*27–29*). In our systems, some fraction of the electrons that are transferred to the surface may be trapped in the metal oxide lattice defects and give rise to the EPR signal. The independence of the value of g1 with type of adsorbate strongly supports the assignment as an F-center in the CuO/silica substrate that was common to all the samples.

Adsorbate PFR Formation. Depending on the number, type, and position of the substituent groups, either one or two types of PFRs were formed. Phenol and hydroquinone are the limiting cases, both forming only one type of radical: a g2-type radical for phenol and g3-type radical for hydroquinone.

Phenol. There is only one hydroxyl substituent to react with the surface, and this reaction should form a phenoxyl radical. (cf. Figure 4, pathway II) The reaction occurs through initial formation of a hydrogen bonding complex followed by chemisorption through elimination of H_2O. Density functional theory (DFT) calculations indicate that phenoxyl radicals can exist as a combination of both oxygen-centered (the electron density of the unpaired electron is concentrated on the oxygen) and carbon-centered (the electron density of the unpaired electron is concentrated on an ortho- or para-carbon) (*36*). These types of radicals are known to have moderately high *g*-values ranging from 2.0030 to 2.0040 (*30*). This is in contrast to F-centers with *g*-values of 2.0011–2.0020 and carbon-centered radicals in soot or polymeric materials

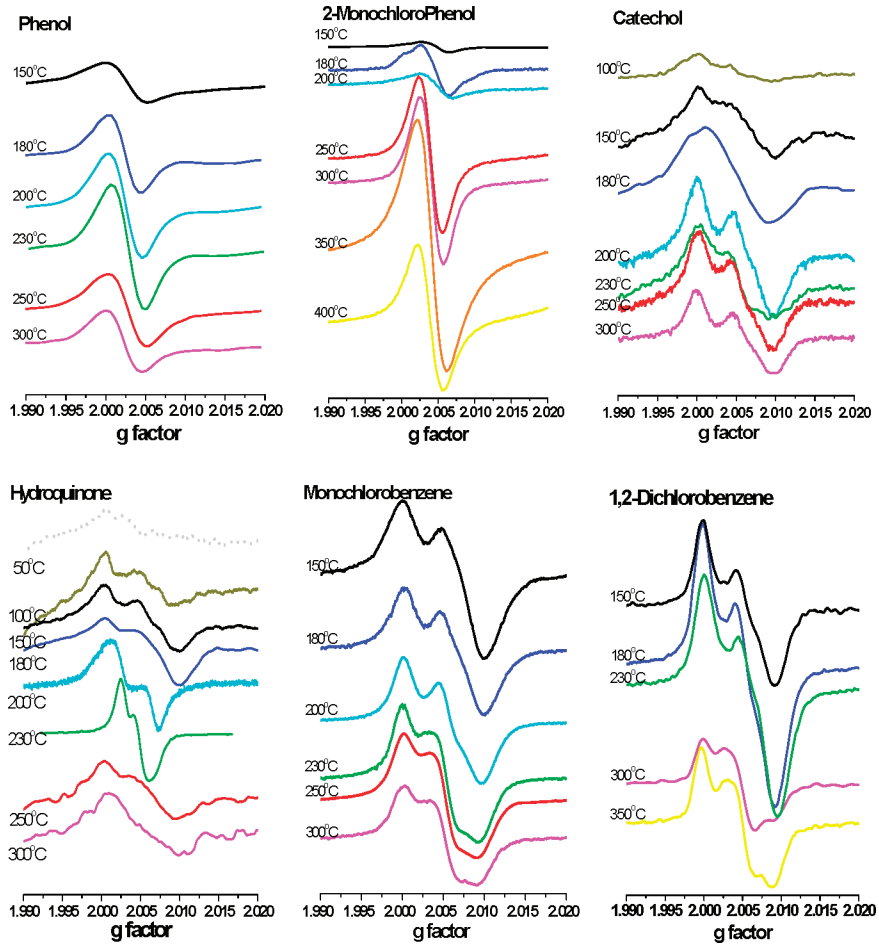

FIGURE 2. Temperature dependence of first derivative EPR spectra of 5% $Cu^{II}O$/silica particles dosed with various radical precursors.

TABLE 1. *g*-Factors of Deconvoluted EPR Spectra at 150 and 300 °C

precursor	g1 (150°C)	g2 (150°C)	g3 (150°C)	g1 (300°C)	g2 (300°C)	g3 (300°C)
2-MCP	2.0018	2.0049		2.0011	2.0041	2.0060
phenol	2.0020	2.0038		2.0011	2.0032	
CT	2.0018		2.0061	2.0014	2.0042	2.0070
HQ	2.0015		2.0065	2.0020		2.0062
MCBz	2.0015		2.0070	2.0016	2.0047	2.0067
1,2-DCBz	2.0013	2.0041	2.0068	2.0010	2.0044	2.0063

with *g*-values usually less than 2.0030 (*27–29*). This is the only type of PFR observed from phenol at all temperatures, with *g*-values ranging from 2.0038 at 150 °C to 2.0035 at 300 °C. Thus, the g2 radical formed from chemisorption of phenol is assigned as a phenoxyl radical.

Hydroquinone. Hydroquinone is *p*-hydroxy-substituted phenol. Hydroquinones chemisorb to the surface by the same mechanism as phenol and form a *p*-semiquinone radical (cf. Figure 4, pathway III) that is known to be highly persistent (*31*). As primarily oxygen-centered radicals, they will have very high *g*-factors, typically greater than 2.0040 (*32*) (and up to 2.011 for some substituted quinones (*33*)). On the basis of what appears to be only one possible reaction product and the high *g*-factor of 2.0064–2.0062 from 150 to 300 °C, the structure of the g3 radical formed from hydroquinone is assigned as that of *p*-semiquinone. This is higher than the value of the semiquinone radical anion in solution that is usually reported to be between 2.0045 and 2.0060 (*34, 35*), the difference being attributed to the interaction with the surface.

1,2-Dichlorobenzene, Catechol, and 2-Monochlorophenol. Two PFR signals were observed for the doubly substituted adsorbates, 1,2-DCBz, CT, and 2-MCP. For *o*-chlorine- and *o*-hydroxy-substituted molecules, chemisorption can occur via reaction with both substituents through elimination of HCl and/or H_2O, respectively. If chemisorption occurs through both groups, the resulting chemisorbed species is an *o*-semiquinone radical. For some *o*-chlorine- or -hydroxy-substitiuted benzenes, we observed formation of two different radicals. In analogy with the discussion of phenol and hydroquinone and depending upon the observed *g*-value, the structures of these two radicals were assigned as either phenoxyl (g2) or semiquinone-type (g3) radicals.

2-Monochlorophenol. 2-MCP forms primarily one radical, a 2-chlorophenoxyl (g2 = 2.0041–2.0049), at lower temperatures but both 2-chlorophenoxyl and *o*-semiquinone (g3 = 2.0060) radicals at higher temperature. The formation of only 2-chlorophenoxyl radical at low temperature is consistent with the more energetically favorable elimination of H_2O over HCl. At higher temperatures, there is sufficient energy to overcome the activation barrier to either process and g3 radicals are also formed (cf. Figure 4, pathway I). The observed g2 values for 2-MCP were higher than those observed for phenol. This is attributed to the presence of a chlorine substitutent for the 2-chlorophenoxyl radical formed from 2-MCP, which increases the spin–orbit coupling constant (due to the heavy atom effect), that increases the g2 value. At higher temperatures, some of the 2-chlorophenoxyl radical may have been dechlorinated leading to reduction in the average g2 value closer to that of phenoxyl.

1,2-Dichlorobenzene. 1,2-DCBz forms both a 2-chlorophenoxyl radical (g2 = 2.0041–2.0044) and an *o*-semi-

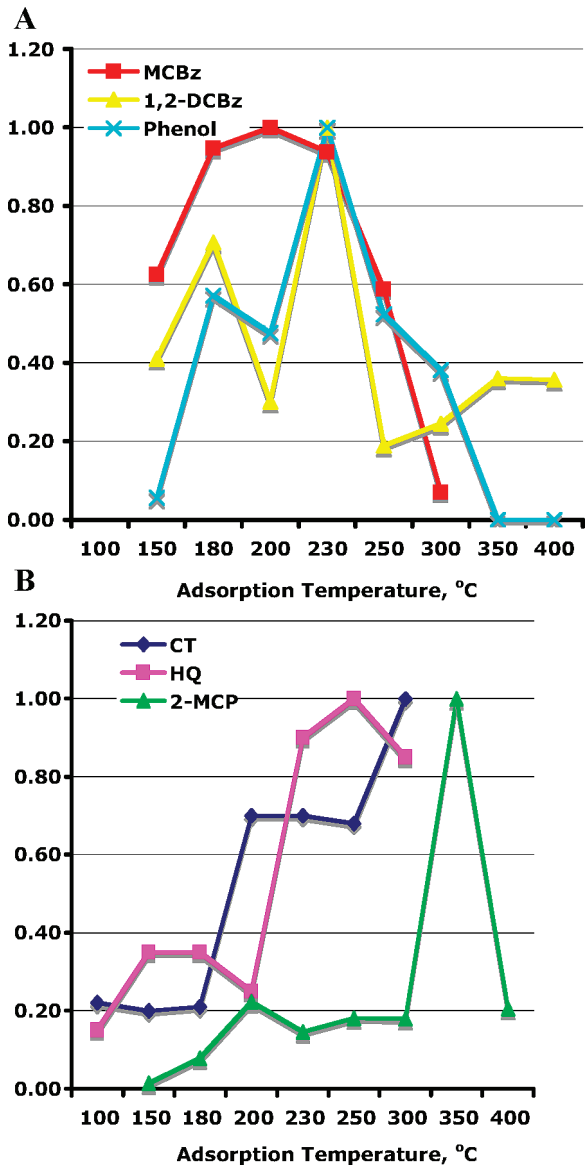

FIGURE 3. Temperature dependence of relative intensities of total PFR signal.

quinone radical (g3 = 2.0063–2.0068) at all temperatures (cf. Figure 4, pathway V). Some adsorption sites favor chemisorption by elimination of a single HCl to form 2-chlorophenoxyl radical while other sites favor double HCl elimination to form *o*-semiquinone radicals. The type of adsorption (single or double elimination) is likely dependent on the availability of the adjacent surface hydroxyl groups and the geometry of the adsorption site. The resulting species have *g*-values in the same range as 2-MCP. The g2 value for the 2-chlorophenoxyl radical was higher than the value for the unsubstituted phenoxyl radical formed by phenol due to the heavy atom effect of chlorine.

Catechol. CT forms only an *o*-semiquinone radical (g3 = 2.0061–2.0070) at low temperature (cf. Figure 4, pathway IV), but both *o*-semiquinone (g3) and phenoxyl (g2 = 2.0042) radicals at high temperature. While chemisorption by the double elimination of two waters is energetically feasible, the resulting semiquinone is subject to surface-mediated degradation leading to the formation of phenoxyl radical as depicted in Figure 5. This degradation of the semiquinone radical to phenoxyl probably also occurs for the semiquinones of 2-MCP and 1,2-DCBz, but it was not easily observable due to the formation of phenoxyl at lower temperatures.

Monochlorobenzene. MCBz exhibits behavior similar to that of 1,2-DCBz and CT by forming mostly semquinone radicals (g3 = 2.0070) at lower temperatures and both g3 and phenoxyl radicals (g2 = 2.0047) at higher temperatures. This was a surprising behavior because one could expect chemisorption of the monosubstituted MCBz to be more similar to the monosubstituted phenol than the doubly substituted CT. However, in separate research on formation of dioxins from chlorinated benzenes, we found that MCBz is readily chlorinated via hypochlorites formed on CuO/silica to form 1,2-DCBz which forms a g3 semiquinone-type radical (*19, 21*). The appearance of the g2 phenoxyl radicals at higher temperatures is again attributed to decomposition of the initially formed *o*-semiquinone radicals.

Temperature Dependence of g2 and g3 Radical *g*-Factors. The values of g3 for all the adsorbates and the g2 for catechol and phenol are relatively constant with temperature; however, the g2 values decrease with increasing temperature for 2-MCP, 1,2-DCBz, and MCBz (cf. Figure 6A). The ratio of g2 to g3 yield increased by a factor of 2–5 with increasing temperature for all the adsorbates for which two types of radicals were formed simultaneously (cf. Figure 6B). Two types of reactions can explain these observations: (1) dechlorination of the initially formed chlorophenoxyl to phenoxyl radical (without the heavy atom effect from the chlorine substituent, the g2 value is 2.0030–2.0040 instead of the 2.0040−2.0050 value with the chlorine substituent) and (2) the surface-mediated decomposition of *o*-semiquinone radical (vide supra) to surface-bound phenoxyl radicals. Both processes decrease the g2 values and increase in the g2 to g3 concentration ratio.

PFR Lifetimes and Persistence. The lifetimes of the various radicals in air are all similar and quite long. (cf. Figure 1) The small differences in lifetimes and the relative persistence of the radicals can be assigned in the order given below:

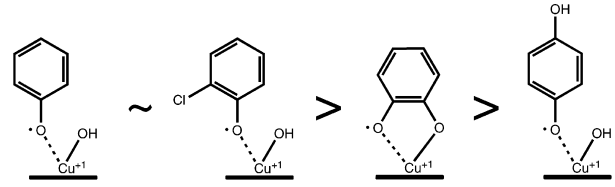

Given the reported persistence of semiquinone-type radicals, it is somewhat surprising that phenoxyl radical and chlorinated phenoxyl radical appear to be more persistent than *o*-semiquinone and *p*-semiquinone radicals. However, they do follow the general trend observed for our calculated reactivities of gas-phase radicals with O_2 (*36*). Ab initio DFT modeling of radicals associated with copper oxide cluster is under way to help elucidate the stabilities of the radicals on metal surfaces.

Environmental and Human Health Implications

Reaction of each adsorbate with $Cu^{II}O$-containing particles results in formation of a radical that neither decomposes nor reacts rapidly with air. The resulting radical is thus environmentally persistent under normal ambient conditions. Each adsorbate that we studied was a combustion-generated chlorine- or hydroxyl-substituted benzene that contained a functional group that could react with surface hydroxyl or oxide groups (*37, 38*). We initially thought that only semiquinone radicals would be environmentally persistent, as they are known for their stability and resistance to oxidation in cigarette smoke (*24*). However, our studies have shown that phenoxyl radicals are just as persistent, at least when associated with $Cu^{II}O$, and both phenoxyl- and

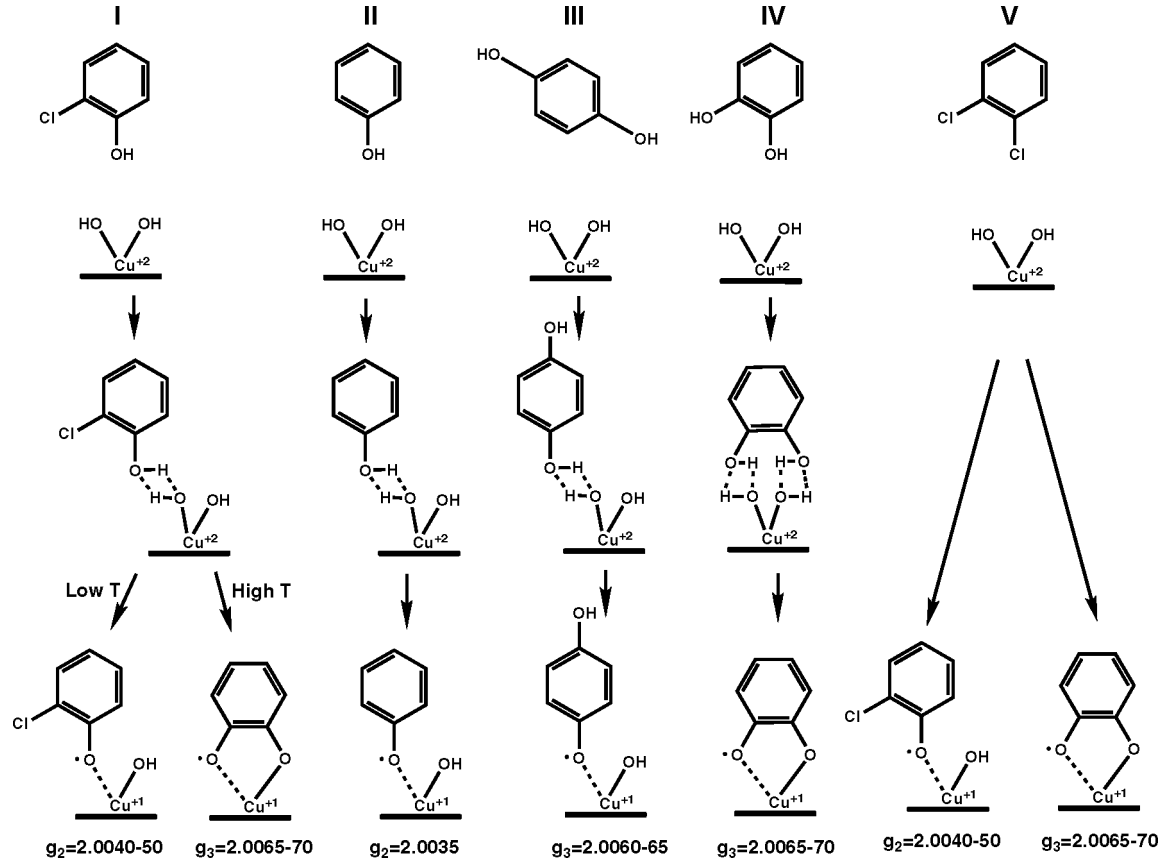

FIGURE 4. Formation of PFRs from various precursors on a Cu(II) surface. The precursors initially physisorb through hydrogen bonding. Chemisorption occurs via H_2O and HCl elimination for the substituted phenols and chlorinated benzenes, respectively. Electron-transfer results in formation of the PFR and Cu(I). When an ortho-substituent is also present, a PFR radical anion can be formed through a second HCl or H_2O elimination reaction with the surface. MCBz immediately forms the same PFR as 1,2-DCBZ through metal catalyzed chlorination.

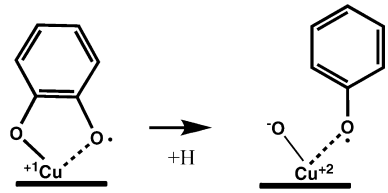

FIGURE 5. Surface decomposition of *o*-semiquinone radicals to form phenoxyl radicals.

semiquinone-type PFRs can be formed from a variety of substituted aromatic precursors. Our formation model can be extended to other redox-active transition metals. In particular, the behavior of iron in surface-assisted PFR formation is of great interest as it is the most abundant transition metal in most PM (*4, 8, 15*).

Our studies were performed under postflame, cool-zone combustion conditions (*20*). The high-temperature flame zone of combustors will form the fine and ultrafine particle substrates. However, the temperature in the flame and postflame zones are too high (>1200 and 600–1200 °C, respectively) for chemisorption to occur, and radicals will decompose rapidly even if they were formed. However, all combustion gases pass through a cool zone (~600 °C to ambient) as they exit the combustor and are emitted from the stack. It is under cool-zone conditions that the PFR/particle systems are formed. Cool-zone conditions exist in essentially every combustor and thermal process. Thus, the types of PFRs discussed in this manuscript have the potential to be formed in a large number of thermal processes and will not be destroyed since they are formed after the flame zone.

Airborne PM2.5 has been reported to contain significant concentration of PFRs (*16, 39*). The EPR spectra of these samples were very complex, probably containing multiple types of PFRs. Our results indicate that the interaction of a very simple molecular species with an active surface can result in formation of more than one type of radical. It is certainly possible that other types of PFRs other than those studied here are formed in combustion systems and are present on airborne PM. Substituted polycyclic aromatic hydrocarbons (PAHs) are almost certain to form PFRs analogous to those formed from substituted benzenes. Other organic molecular species may react with transition metals to form PFRs through direct formation of the PFR of the initial molecular species or through chemisorption and surface-mediated reaction to form higher molecular weight aromatic species that then form additional PFRs. Initially formed PFRs may also slowly rearrange or react to form chemically new PFRs.

The biological impact of PFRs revolves around their ability to generate oxidative stress. Semiquinone-type radicals are suspected to catalyze or mediate formation of ROS that can initiate cardiopulmonary disease or cancer by variously proposed, but poorly understood, mechanisms (*5, 12, 40*). Most of the published research to date has focused on the role of Fe^{2+} in fine particles on the formation of ROS through the Fenton reaction (*13*). However, transition metals in fine particles exist almost exclusively in their higher oxidation states (e.g., Fe(III) and Cu(II), rather than Fe(II) and Cu(I)) and are not mobile in

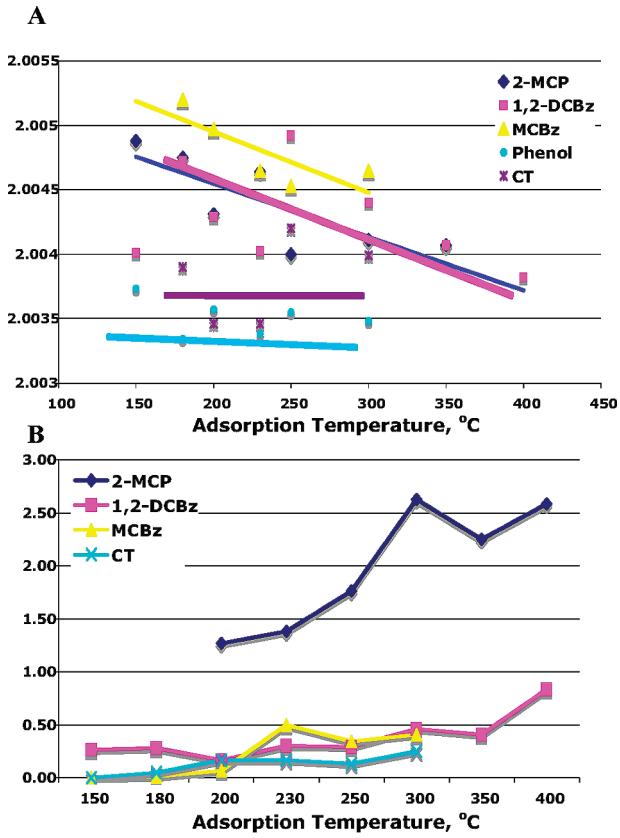

FIGURE 6. Temperature dependence of *g*-factors of g2 and g3 radicals: (A) variation of g2-factors with losing temperature; (B) ratio of concentration of g2 to g3 radicals.

biological solutions as would be required for solution redox chemistry (*13*). Furthermore, the semiquinone hypothesis for formation of ROS proposed in the literature involves a cycle in which a semiquinone radical anion reacts with molecular oxygen to form superoxide that then reacts with biological reducing equivalents such as NADPH and ascorbate to form hydrogen peroxide that disproportionates into hydroxyl radical and hydroxide in a Fenton reaction involving endogenous Fe^{2+} (*13*). Hydroquinones and quinones are involved in a cycle that regenerates the semiquinone radical anion.

However, this model does not address how semiquinones are delivered to the biological system nor how exogenous transition metals may be involved in the ROS-generating cycles (*41*). The particle-associated PFR/transition metal system described herein addresses these issues and appears to be a very efficient system for inducing ROS and oxidative stress in exposed organisms.

Acknowledgments

We gratefully acknowledge the partial support of this work under NSF NIRT grant CTS-0404314 and NSF Grant CTS-0625548 as well as the Patrick F. Taylor Chair Foundation.

Supporting Information Available

Figures A−C along with additional information about EPR spectral deconvolution and PCR Yields. This material is available free of charge via the Internet at http://pubs.acs.org.

Literature Cited

(1) Dockery, D. W.; Pope, C. A., 3rd; Xu, X.; Spengler, J. D.; Ware, J. H.; Fay, M. E.; Ferris, B. G., Jr.; Speizer, F. E. An association between air pollution and mortality in six U.S. cities. *N. Engl. J. Med.* **1993**, *329* (24), 1753–9.

(2) Pope, C. A.; Burnett, R. T.; Thun, M. J.; Calle, E. E.; Krewski, D.; Ito, K.; Thurston, G. D. Lung cancer, cardiopulmonary mortality, and long-term exposure to fine particulate air pollution. *JAMA, J. Am. Med. Assoc.* **2002**, *287* (9), 1132–1141.

(3) Harrison, R. M.; Shi, J. P.; Xi, S.; Khan, A.; Mark, D.; Kinnersley, R.; Yin, J. Measurement of number, mass and size distribution of particles in the atmosphere. *Philos. Trans. R. Soc. London, Ser. A: Math., Phys. Eng. Sci.* **2000**, *358* (1775), 2567–2580.

(4) Nielsen, M. T.; Livbjerg, H.; Fogh, C. L.; Jensen, J. N.; Simonsen, P.; Lund, C.; Poulsen, K.; Sander, B. Formation and emission of fine particles from two coal-fired power plants. *Combust. Sci. Technol.* **2002**, *174* (2), 79–113.

(5) Peters, A.; Dockery, D.; Muller, J.; Mittleman, M. Increased particulate air pollution and the triggering of myocardial infarction. *Circulation* **2001**, *103* (23), 2810–2815.

(6) Nel, A. Air pollution-related illness: Effects of particles. *Science* **2005**, *308* (5723), 804–806.

(7) Kennedy, I. M. The health effects of combustion-generated aerosols. *Proc. Combust. Inst.* **2007**, *31* (2), 2757–2770.

(8) Cass, G. R.; Hughes, L. A.; Bhave, P.; Kleeman, M. J.; Allen, J. O.; Salmon, L. G. The chemical composition of atmospheric ultrafine particles. *Philos. Trans. R. Soc. London, Ser. A: Math., Phys. Eng. Sci.* **2000**, *358* (1775), 2581–2592.

(9) Lighty, J. S.; Veranth, J. M.; Sarofim, A. F. Combustion aerosols: Factors governing their size and composition and implications to human health. *J. Air Waste Manage. Assoc.* **2000**, *50* (9), 1565–1618.

(10) Allouis, C.; Beretta, F.; D'Alessio, A. Structure of inorganic and carbonaceous particles emitted from heavy oil combustion. *Chemosphere* **2003**, *51* (10), 1091–1096.

(11) Gurgueira, S. A.; Lawrence, J.; Coull, B.; Murthy, G. G. K.; Gonzalez-Flecha, B. Rapid increases in the steady-state concentration of reactive oxygen species in the lungs and heart after particulate air pollution inhalation. *Environ. Health Perspect.* **2002**, *110* (8), 749–755.

(12) Valavanidis, A.; Fiotakis, K.; Bakeas, E.; Vlahogianni, T. Electron paramagnetic resonance study of the generation of reactive oxygen species catalysed by transition metals and quinoid redox cycling by inhalable ambient particulate matter. *Redox Rep.* **2005**, *10* (1), 37–51.

(13) Halliwell, B.; Gutteridge, J. M. C. *Free Radicals in Biology and Medicine*; Oxford University Press: New York, 1999.

(14) Knaapen, A. M.; Shi, T. M.; Borm, P. J. A.; Schins, R. P. F. Soluble metals as well as the insoluble particle fraction are involved in cellular DNA damage induced by particulate matter. *Mol. Cell. Biochem.* **2002**, *234* (1), 317–326.

(15) Kukier, U.; Ishak, C. F.; Sumner, M. E.; Miller, W. P. Composition and element solubility of magnetic and non-magnetic fly ash fractions. *Environ. Pollut.* **2003**, *123* (2), 255–266.

(16) Dellinger, B.; Pryor, W. A.; Cueto, R.; Squadrito, G. L.; Deutsch, W. A. Combustion-generated radicals and their role in the toxicity of fine particulate. *Organohalogen Compd.* **2000**, *46*, 302–305.

(17) Pryor, W. A.; Hales, B. J.; Premovic, P. I.; Church, D. F. The radicals in cigarette tar-Their nature and suggested physiological implications. *Science* **1983**, *220* (4595), 425–427.

(18) Kumagai, Y.; Arimoto, T.; Shinyashiki, M.; Shimojo, N.; Nakai, Y.; Yoshikawa, T.; Sagai, M. Generation of reactive oxygen species during interaction of diesel exhaust particle components with NADPH-cytochrome P450 reductase and involvement of the bioactivation in the DNA damage. *Free Radical Biol. Med.* **1997**, *22* (3), 479–487.

(19) Lomnicki, S.; Dellinger, B. A detailed mechanism of the surface-mediated formation of PCDD/F from the oxidation of 2-chlorophenol on CuO/silica surface. *J. Phys. Chem. A* **2003**, *107*, 4387–4395.

(20) Cormier, S. A.; Lomnicki, S.; Backes, W.; Dellinger, B. Origin and health impacts of emissions of toxic by-products and fine particles from combustion and thermal treatment of hazardous wastes and materials. *Environ. Health Perspect.* **2006**, *114* (6), 810–817.

(21) Lomnicki, S.; Dellinger, B. Formation of PCDD/F from the pyrolysis of 2-chlorophenol on the surface of disperced copper oxide particles. *Proc. Combust. Inst.* **2002**, *29*, 2463–2468.

(22) Born, J. G. P.; Louw, R.; Mulder, P. Fly ash mediated (oxy)chlorination of phenol and its role in PCDD/F formation. *Chemosphere* **1993**, *26* (12), 2087–95.

(23) Weber, R.; Dinjus, E.; Stieglitz, L. The role of copper(II) chloride in the formation of organic chlorine in fly ash. *Chemosphere* **2001**, *42*, 579–582.

(24) Pryor, W. A.; Prier, D. G.; Church, D. F. Electron-spin resonance study of mainstream and sidestream cigarette-smoke-Nature

of the free-radicals in gas-phase smoke and in cigarette tar. *Environ. Health Perspect.* **1983**, *47* (1), 345–355.
(25) Alderman, S. L.; Dellinger, B. FTIR investigation of 2-chlorophenol chemisorption on a silica surface from 200 to 500 °C. *J. Phys. Chem. A* **2005**, *109*, 7725–7731.
(26) Alderman, S. L.; Farquar, G. R.; Poliakoff, E. D.; Dellinger, B. An infrared and X-ray spectroscopic study of the reactions of 2-chlorophenol, 1,2-dichlorobenzene, and chlorobenzene with model CuO/silica fly ash surfaces. *Environ. Sci. Technol.* **2005**, *39* (19), 7396–7401.
(27) Richards, R. M.; Volodin, A. M.; Bedilo, A. F.; Klabunde, K. J. ESR study of nanocrystalline aerogel-prepared magnesium oxide. *Phys. Chem. Chem. Phys.* **2003**, *5* (19), 4299–4305.
(28) Pena, O.; Rodriguez-Fernandez, L.; Cheang-Wong, J. C.; Santiago, P.; Crespo-Sosa, A.; Munoz, E.; Oliver, A. Characterization of nanocluster formation in Cu-implanted silica: Influence of the annealing atmosphere and the ion fluence. *J. Non-Cryst. Solids* **2006**, *352* (4), 349–354.
(29) Di Valentin, C.; Neyman, K. M.; Risse, T.; Sterrer, M.; Fischbach, E.; Freund, H. J.; Nasluzov, V. A.; Pacchioni, G.; Rosch, N. Density-functional model cluster studies of EPR g tensors of F-s(+) centers on the surface of MgO. *J. Chem. Phys.* **2006**, *124*, 044708.
(30) Boyd, S. A.; Mortland, M. M. Dioxin radical formation and polymerization on Cu(Ii)-smectite. *Nature* **1985**, *316* (6028), 532–535.
(31) Stone, K.; Pryor, W. A. Analysis and fractionation of cigaret tar extracts: What causes DNA damage? *Book of Abstracts, 216th ACS National Meeting, Boston, Aug. 23–27, 1998*; American Chemical Society: Washington, D.C., 1998; AGFD-178.
(32) Neta, P.; Fessende, R. W. Hydroxyl radical reactions with phenols and anilines as studied by electron-spin resonance. *J. Phys. Chem.* **1974**, *78*, 523–529.
(33) Hosaka, H.; Meguro, K.; Kawashim, N. Estimation of surface properties of metal-oxides by use of Tcnq adsorption. 2. Electron-donor property of silica-alumina, silica-titania, and alumina-titania system Ssurfaces. *Bull. Chem. Soc. Jpn.* **1972**, *45* (11), 3371–3375.
(34) Yonezawa, T.; Kawamura, T.; Ushio, M.; Nakao, Y. Solvent effects on G-factors of semiquinones. *Bull. Chem. Soc. Jpn.* **1970**, *43* (4), 1022.
(35) Hales, B. J.; Case, E. E. Immobilized radicals. 4. Biological semiquinone Anions and neutral semiquinones. *Biochim. Biophys. Acta* **1981**, *637* (2), 291–302.
(36) Dellinger, B.; Lomnicki, S.; Khachatryan, L.; Maskos, Z.; Hall, R. W.; Adounkpe, J.; McFerrin, C.; Truong, H. Formation and stabilization of persistent free radicals. *Proc. Combust. Inst.* **2007**, *31* (1), 521–528.
(37) Weber, R.; Hagenmaier, H. PCDD/PCDF formation in fluidized bed incineration. *Chemosphere* **1999**, *38* (11), 2643–2654.
(38) Blumenstock, M.; Zimmermann, R.; Schramm, K.-W.; Kaune, A.; Nikolai, U.; Lenoir, D.; Kettrup, A. Estimation of the dioxin emission (PCDD/FI-TEQ) from the concentration of low chlorinated aromatic compounds in the flue and stack gas of a hazardous waste incinerator. *J. Anal. Appl. Pyrolysis* **1999**, *49* (1–2), 179–190.
(39) Dellinger, B.; Pryor, W. A.; Cueto, R.; Squadrito, G. L.; Hegde, V.; Deutsch, W. A. Role of free radicals in the toxicity of airborne fine particulate matter. *Chem. Res. Toxicol.* **2001**, *14* (10), 1371–1377.
(40) Halliwell, B.; Gutteridge, J. M. C. Role of free-radicals and catalytic metal-ions in human-disease-An overview. *Methods Enzymol.* **1990**, *186*, 1–85.
(41) Squadrito, G. L.; Cueto, R.; Dellinger, B.; Pryor, W. A. Quinoid redox cycling as a mechanism for sustained free radical generation by inhaled airborne particulate matter. *Free Radical Biol. Med.* **2001**, *31* (9), 1132–1138.

ES071708H